Effect of shear flow on the turbidity of a critical colloidal dispersion

Henk Verduin and Jan K. G. Dhont
Van 't Hoff Laboratory, Utrecht University, Padualaan 8, 3584 CH Utrecht, The Netherlands
(Received 2 February 1995)

Experiments concerning the effect of shear flow on the turbidity of a colloidal dispersion close to its gas-liquid critical point are described. Theory predicts that in the mean-field region, the turbidity of the sheared system relative to that of the quiescent dispersion is a function of a single dimensionless group λ that is proportional to $\dot{\gamma}\xi^{-4}$ ($\dot{\gamma}$ is the shear rate and ξ^{-1} is the correlation length of the quiescent dispersion at the given temperature). Experiments are found to be in accordance with this scaling behavior. Moreover, the experiments confirm the theoretically predicted λ dependence. As a model colloidal system, we used spherical silica particles coated with stearyl alcohol. When dissolved in benzene, these colloidal particles attract each other, due to the fact that benzene is a marginal solvent for the stearyl coating. These attractions give rise to a gas-liquid critical point.

PACS number(s): 82.70.Dd, 05.70.Jk, 83.20.Hn

I. INTRODUCTION

Two well separated particles attain a large relative velocity when subjected to shear flow. With increasing distance (in the gradient direction), a smaller shear rate is sufficient to sustain a given relative velocity. For these large separations, diffusion is never fast enough to restore the shear induced displacements. As a result, extended structures are severely affected by shear flow, even for small shear rates. In particular, close to the gas-liquid critical point, where microstructures exist with linear dimensions of the (ultimately diverging) correlation length, strong influence of weak shear flows is to be expected. This effect is even enhanced, due to a decrease of the diffusion coefficient, commonly referred to as critical slowing down.

The shear rate dependence of the turbidity reflects, in an integrated form, the effect of shear flow on the long-ranged microstructure of a suspension. This shear rate dependence is singular at the critical point. That is, an *infinitesimally* small shear rate is then sufficient to induce a *finite* effect on the turbidity, due to the *infinite* extent of microstructures.

In a recent paper [1] we described the effect of a shear flow on critical correlations in a colloidal system, on the basis of the Smoluchowski equation. This is the equation of motion for the probability density function of the position coordinates of the Brownian particles in the sheared system. The theory is valid in the mean-field region where the equilibrium structure factor attains the Ornstein-Zernike form.

The main result is a relatively simple expression for the structure factor, which is anisotropic and is a highly nonlinear function of the shear rate: this is the Ornstein-Zernike structure factor for a sheared system. We showed that both the effects of shear rate and temperature are described by a single dimensionless group λ which is proportional to $\dot{\gamma}\xi^{-4}$ ($\dot{\gamma}$ is the shear rate and ξ^{-1} is the correlation length in the unsheared system). Calculations of Onuki and Kawasaki [2] and Oxtoby [3] predict a $\dot{\gamma}\xi^{-3}$ scaling beyond the mean-field region for molecular and atomic systems. This kind of scaling implies, as expected, that the effect of a small shear rate is large in the vicinity of the critical point where the correlation length is large.

An important quantity derived from the shear distorted structure factor is the turbidity. The change in turbidity, due to shear flow, is theoretically predicted to be proportional to a scaling function $T(\lambda)$. This scaling function is sharply decreasing with increasing λ, showing that small shear rates have a large effect on the turbidity near the critical point.

We are not aware of experimental data on the influence of shear flow on critical colloidal dispersions. Experiments of this kind have been performed for binary fluids, reported by Beysens and co-workers [4,5]. Their results indicate the same shear rate dependence as predicted for colloidal systems (see Ref. [1]).

The aim of this paper is to verify experimentally the above mentioned scaling for a colloidal dispersion. As a model system we used colloidal silica particles coated with a dense organic layer. Dissolved in a poor solvent for the organic layer, the system exhibits an upper-critical point. We performed transmission experiments, at various shear rates and temperatures in the stable region of the phase diagram in the vicinity of the critical point.

This paper is organized as follows. In the theoretical section we summarize the Smoluchowski equation approach to obtain the shear distorted structure factor, and from that, the shear rate dependence of the turbidity. We also discuss how to obtain the temperature dependence of the correlation length and the Cahn-Hilliard square-gradient coefficient from the equilibrium structure factor.

The experimental section contains a description of the colloidal system and the setup used for the measurement of the small angle critical part of the structure factor and of the shear rate dependence of the turbidity. In the subsequent section the results are presented and discussed. We close with a summary and conclusions.

II. THEORY

A. Effect of a stationary shear flow on microstructure

The influence of a shear flow on the microstructure of a critical colloidal system can be calculated from the equation of motion for the pair-correlation function. This equation is obtained from the N-particle Smoluchowski equation by integration over all, except for two position coordinates [6]. Disregarding hydrodynamic interactions, one obtains the following (stationary) equation of motion for the pair-correlation function g:

$$\frac{\partial}{\partial t}g(\boldsymbol{R}\,|\dot\gamma)=0=2D_0\left[\nabla^2 g(\boldsymbol{R}\,|\dot\gamma)+\beta\nabla\cdot g(\boldsymbol{R}\,|\dot\gamma)\left\{\nabla V(R)+\bar\rho\int d\mathbf{r}[\nabla_r V(r)]\frac{g_3(\mathbf{r},\boldsymbol{R}\,|\dot\gamma)}{g(\boldsymbol{R}\,|\dot\gamma)}\right\}\right]-\nabla\cdot[g(\boldsymbol{R}\,|\dot\gamma)\Gamma\boldsymbol{R}]\ , \tag{1}$$

where D_0 is the Stokes-Einstein diffusion coefficient, $\beta=1/k_BT$, k_B is Boltzmann's constant and T the temperature, V is the pair potential, $\boldsymbol{R}$ denotes the separation between two particles, $\bar\rho$ is the number density N/V, and Γ is the velocity gradient tensor, for which we will take the following form:

$$\Gamma=\dot\gamma\begin{bmatrix}0&1&0\\0&0&0\\0&0&0\end{bmatrix}\ , \tag{2}$$

with $\dot\gamma$ the shear rate. This choice corresponds to a flow in the x direction with its gradient in the y direction.

The three-particle correlation function g_3 is essential for the description of long-range correlations: the integral in Eq. (1) represents the force between two particles which is mediated via other particles. This indirect force becomes long ranged as the critical point is approached, leading to a divergent correlation length ξ^{-1}. Equation (1) is closed by an improved superposition approximation. The asymptotic solution of Eq. (1) for large distances is obtained by Fourier transformation after linearization with respect to the total correlation function $h=g-1$. The relative structure factor distortion is found to be equal to

$$\begin{aligned}\Psi(\boldsymbol{K}\,|\lambda)&\equiv\frac{S(\boldsymbol{K}\,|\lambda)-S^{\rm eq}(K)}{S^{\rm eq}(K)-1}\\&=\frac{1}{\lambda K_1}\int_{K_2}^{\pm\infty}dX(K^2-K_2^2+X^2)(K_2^2-X^2)\\&\qquad\times\exp\left[-\frac{F(\boldsymbol{K}\,|X)}{\lambda K_1}\right]\ ,\end{aligned} \tag{3}$$

where $\boldsymbol{K}=\boldsymbol{k}\xi^{-1}$ is a dimensionless wave vector with Cartesian components K_j, $S(\boldsymbol{K}\,|\lambda)$ is the distorted structure factor, and $S^{\rm eq}(K)$ is the Ornstein-Zernike equilibrium structure factor. The function F is equal to

$$\begin{aligned}F(\boldsymbol{K}\,|X)\equiv&(X-K_2)(K^2-K_2^2)(1+K^2-K_2^2)\\&+\tfrac{1}{3}(X^3-K_2^3)(1+2K^2-2K_2^2)+\tfrac{1}{5}(X^5-K_2^5)\ .\end{aligned} \tag{4}$$

Note that the solution is only a function of two variables: $\boldsymbol{K}$ and λ. The parameter λ describes both the effect of shear and the distance from the critical point through the correlation length ξ^{-1} in the equilibrium system. Large values of λ result in large relative distortions. Thus the effect of decreasing the distance from the critical point (increase of the correlation length) can also be realized by an increase of the shear rate at a constant distance from the critical point. The parameter λ is defined as follows:

$$\lambda=\frac{{\rm Pe}^0(\dot\gamma)}{(\xi R_V)^4(\beta\Sigma/R_V^2)}\ , \tag{5}$$

where the Péclet number ${\rm Pe}^0$ equals $\dot\gamma R_V^2/2D_0$ and R_V is the range of the pair potential. Σ is a well behaved function of the density and the temperature and is related to the Cahn-Hilliard square-gradient coefficient. An important feature is the proportionality of λ with $\dot\gamma\xi^{-4}$. This implies that, close to the critical point, where the correlation length becomes large, a very small shear rate results in a relatively large distortion. Furthermore, as λ always occurs as a product with K_1, there is no distortion in directions where $K_1=0$.

Equation (3) is the Ornstein-Zernike structure factor for a sheared system. Its validity is restricted to the mean-field region, as a result of the linearization of the equation of motion with respect to the total correlation function. Nonlinear terms must be included to go beyond the mean-field region.

In the present paper our special interest is in the shear rate dependence of the turbidity. Integration of Eq. (3) yields an expression for the turbidity under shear flow, relative to the zero shear turbidity,

$$\tau(\dot\gamma)-\tau^{\rm eq}=\frac{C}{(k_0R_V)^2}\frac{1}{(\beta\Sigma/R_V^2)}T(\lambda)\ , \tag{6}$$

where $k_0=2\pi/\lambda_s$, with λ_s the wavelength of the light in the solvent. The function $T(\lambda)$ is defined as

$$T(\lambda)=\int_0^{2\pi}d\phi\int_0^{\infty}dK\frac{K}{1+K^2}\Psi^*(K,\phi|\lambda)\ , \tag{7a}$$

with

$$\Psi^*(K,\phi|\lambda)=\Psi(\boldsymbol{K}=K[\cos\phi,\sin\phi,0]|\lambda)\ . \tag{7b}$$

K, ϕ, and θ are the spherical coordinates of $\boldsymbol{K}$, with the direction of the laser beam chosen along the z axis. The higher order dependence of K on θ in Eq. (7) is neglected, as the structural changes occur at small angles θ. In the derivation of Eqs. (6) and (7) it is assumed that the form factor of the spherical particles is equal to unity over the wave-vector range pertaining to the critical microstruc-

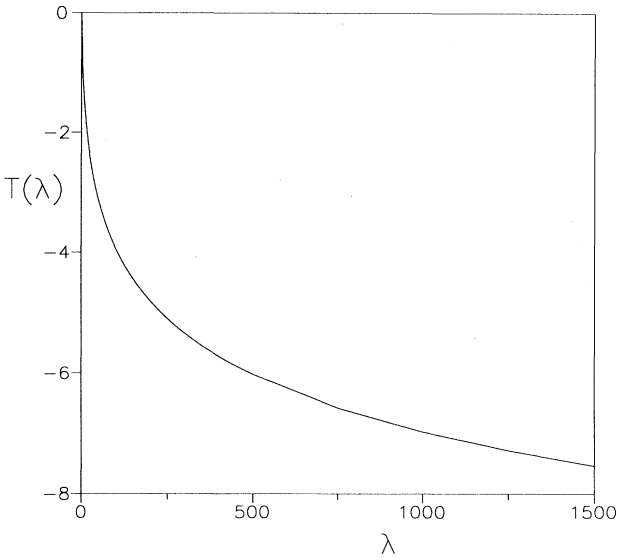

FIG. 1. The turbidity scaling function.

ture. The function $T(\lambda)$ is calculated from Eqs. (3) and (4) by numerical integration, and is plotted in Fig. 1. The constant C appearing in Eq. (6) is related to the optical contrast between the particles and the solvent,

$$C=\frac{4\pi^4 k_0^4}{(2\pi)^6\varepsilon_s^2}\bar{\rho}\left[\int_{V_d} dr[\varepsilon(r)-\varepsilon_s]\right]^2, \tag{8}$$

where V_d is the volume of a colloidal particle and $\varepsilon(r)$ and ε_s are the dielectric constants of the particle and the solvent, respectively.

Equation (6) is the relation we wish to verify experimentally. Measurements of $\tau(\dot{\gamma})-\tau^{eq}$ plotted as a function of $\dot{\gamma}\xi^{-4}$ should all collapse on a single curve. Notice that identical numerical values of $\dot{\gamma}\xi^{-4}$ may correspond to different shear rates and temperatures. Moreover, when the proportionality factors relating $\tau(\dot{\gamma})-\tau^{eq}$ to $T(\lambda)$ in Eq. (6), and relating $\dot{\gamma}\xi^{-4}$ to λ to Eq. (5) are known, all the data points should coincide with the master curve plotted in Fig. 1. To perform this mapping we must determine the temperature dependence of the correlation length ξ^{-1} in the equilibrium system and a value for Σ. The next section is a discussion on how to obtain the correlation length and Σ from the equilibrium structure factor.

B. Determination of the correlation length

One way to obtain experimentally the correlation length in the equilibrium system is by means of light scattering. The equilibrium structure factor derived from Eq. (1) has the well known Ornstein-Zernike form,

$$S^{eq}(k)=\frac{(\beta\Sigma)^{-1}+k^2}{k^2+\xi^2}\ . \tag{9}$$

The measured scattered intensity is directly proportional to $S^{eq}(k)$. Our interest is in the critical short wave-vector contribution to the scattered intensity. To correct for noncritical contributions to the small wave-vector scattered intensity, resulting from short-ranged interactions, the noncritical zero-wave-vector contribution to the structure factor, $S_{nc}^{eq}(0)$, is subtracted from Eq. (9). In an experiment this is done in approximation, by subtraction of the high-temperature intensities from the measured low-temperature intensities, yielding a net intensity. The reciprocal net intensity is given by

$$I_{net}^{-1}\propto\frac{k^2+\xi^2}{(\beta\Sigma)^{-1}-S_{nc}^{eq}(0)\xi^2-[S_{nc}^{eq}(0)-1]k^2}\ . \tag{10}$$

For small wave vectors, where $(k\xi)^2\ll 1$, the quotient of the intercept and slope of a plot of the reciprocal net intensity versus k^2 yields ξ^2. Moreover, from a plot of the reciprocal slopes versus ξ^2, a value for $(\beta\Sigma)S_{nc}^{eq}(0)$ can be extracted. Estimation of $S_{nc}^{eq}(0)\approx 1$ then yields an estimate for $\beta\Sigma$, which quantity is directly proportional to the Cahn-Hilliard square-gradient coefficient.

A second way to obtain the correlation length is via the turbidity [7]. The correlation length dependence of the turbidity is obtained by integration of $I(k)$ over the unit sphere. The intensity equals $CP(k)S^{eq}(k)$ with $P(k)$ the form factor of a sphere,

$$P(k)=\left[3\frac{\sin(ka)-ka\cos(ka)}{(ka)^3}\right]^2$$
$$=1-\tfrac{1}{5}(ka)^2+\tfrac{6}{350}(ka)^4+O((ka)^6)\ . \tag{11}$$

The Taylor expansion makes it possible to perform the integration analytically. The result for the turbidity in terms of $\alpha=2(k_0\xi^{-1})^2$ is

$$\tau(\alpha)\propto\alpha\left[\frac{2\alpha^2+2\alpha+1}{\alpha^3}\ln(1+2\alpha)-2\frac{(1+\alpha)}{\alpha^2}-\tfrac{2}{5}a^2k_0^2\left\{\frac{2\alpha^2+2\alpha+1}{\alpha^4}\ln(1+2\alpha)-\frac{(8/3)\alpha^2+2\alpha+2}{\alpha^3}\right\}\right.$$
$$\left.+\tfrac{12}{175}a^4k_0^4\left\{\frac{2\alpha^2+2\alpha+1}{\alpha^5}\ln(1+2\alpha)-\frac{\frac{8}{3}\alpha^3+\frac{8}{3}\alpha^2+2\alpha+2}{\alpha^3}\right\}+O((ak_0)^6)\right]\ . \tag{12}$$

The experimentally obtained turbidity as a function of the temperature can be fitted to Eq. (12). The relation between the correlation length and the temperature is then parametrized as

$$\xi^{-1}=\xi_0^{-1}(T-T_c)^{-\nu} \tag{13}$$

where ν is the critical exponent, ξ_0^{-1} is a prefactor, and T_c is the critical temperature. Higher order terms in ak_0

are omitted in Eq. (12): for the colloidal system used in the present study the numerical value of ak_0 is ≈ 0.4, so that higher order terms in Eq. (12) are indeed negligible.

III. EXPERIMENT

A. The colloidal system

The colloidal system consists of spherical silica particles coated with stearyl alcohol [8]. The radius determined in cyclohexane at low concentration with dynamic and static light scattering is 39 ± 1 nm. The size polydispersity is about 12%. The specific volume (q) was determined from the relative viscosity, η_r, at low mass concentration. Using Einstein's law [9], which states that $\eta_r = 1 + 2.5\phi$, with ϕ the volume fraction ($=qc$, and c the mass concentration), we obtained $q = 0.69$ cm^3/g. This value was used to calculate volume fractions from known mass concentrations. Mass concentrations were determined by drying a known volume of the silica dispersion for several hours until no change in the mass was recorded.

The interaction between the particles depends on the quality of the solvent. In cyclohexane, which is good solvent for the stearyl alcohol, the spheres behave effectively as hard spheres. Dissolved in benzene, which is a poor solvent for the stearyl alcohol coating, an attractive interaction is induced which increases with decreasing temperature. Due to the short length of the stearyl alcohol chains (about 2 nm) the attractive part of the pair potential is of short range. The pair interaction potential can therefore be modeled with a square well potential of which the depth increases with decreasing temperature [10]. Above the θ temperature for stearyl in benzene, the depth of the square well is zero and the particles behave as hard spheres. When the temperature is lowered significantly, the attractive forces induce phase separation.

The determination of the phase diagram of this colloidal system is extensively described in Ref. [11]. Three different types of phase transition lines are found: the binodal, spinodal, and the gelline (see Fig. 2). For volume fractions smaller than 0.19, the gel transition is located below the binodal and spinodal. At volume fractions larger than 0.19, the gelline masks the binodal and spinodal. We observed an upper-critical point at a volume fraction of 0.19. All experiments described here were performed at this volume fraction. The critical temperature obtained from cloud point measurements is 17.95 °C.

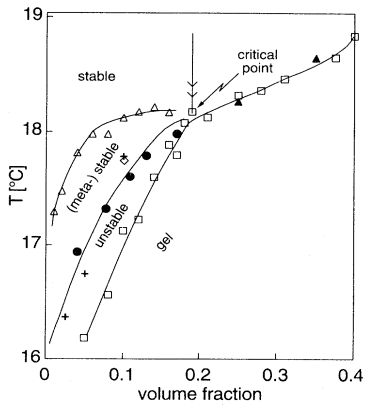

FIG. 2. Phase diagram of the colloidal dispersion. The different phases are indicated.

B. Structure factor measurements

The equilibrium structure factor is obtained from small angle light scattering experiments. For detection we used a diode camera consisting of 512 diodes with a dynamic resolution of 10^{14} and an accuracy of 5% (EG&G/Princeton Applied Research model 1452A). To improve on the accuracy, the intensities of ten adjacent diodes were averaged. The camera's diode chip covered an angle range from 2.9° to 7.4°. As a light source we used a He-Ne laser with a wavelength of 632.8 nm. The experimental ka range is thus 0.029 to 0.075 (k is the wave vector and a is the particle radius). The camera is interfaced to a microcomputer for data control.

To suppress effects of multiple scattering, the sample was sealed in a thin flat 0.2 mm cuvette. The samples were made dust free by centrifugation for 10 min at a speed of 2000 rpm. The cuvette was immersed in a thermostated toluene bath with an optical cylindric glass wall, the temperature of which was measured with a Pt-100 element. Scattering angle dependent intensities were measured at 20 different temperatures ranging from 19 °C to 18 °C.

C. Shear rate dependence of the turbidity

Measurements of the shear rate dependence of the turbidity were performed in a shear cell specially designed for this purpose [12]. The cell consists of two concentric cylinders made of optical glass. The gap between the inner and outer cylinder is 1.0 mm. The outer cylinder is doubly walled for temperature control by water circulation. Two windows are left single for optical use. The outer cylinder is clamped between two stainless steel plates at the top and at the bottom. Both plates are hollow for temperature control by water circulation. Evaporation is diminished by means of a waterlock. The temperature was measured by a Pt-100 resistance element which was installed in the bottom plate. A spindle, fastened on the inner cylinder, was connected to an electromotor for shear rate control. Shear rates ranged from 0.3 to 1000 s^{-1}.

A He-Ne laser beam (632.8 nm) was directed through the center of the inner cylinder perpendicular to the flow and vorticity direction. On both sides of the cell the laser beam passed a pinhole to ensure that no scattered light at very small angles is detected. The intensity of the laser beam was regulated by means of two polarizing filters. A photocell was used for detection. At each different shear rate the transmittance for various temperatures was measured. In the low shear rate regime more data were taken, as large effects are expected for small shear rates close to the critical point. From the solvent corrected transmittance data, the turbidity for each shear rate and

temperature was then calculated from the Lambert-Beer law.

The temperature dependent zero shear turbidity was obtained by slowly cooling down the dispersion at a rate of 0.25 °C/h, starting at a temperature of 21 °C down to 17 °C. We verified that the rate of cooling does not affect the measured temperature dependence of the turbidity.

IV. RESULTS

A. Equilibrium correlation length

In Fig. 3 the experimental reciprocal net intensities are plotted as a function of k^2, for ten different temperatures. The solid lines in the figure represent linear fits. A few temperatures are omitted from this plot for clarity. The intercept decreases with decreasing temperature, while the slopes remain more or less unchanged. From Eq. (10) it follows that these slopes are proportional to $1/[(\beta\Sigma)^{-1}-\xi^2]$, provided that $S_{nc}^{eq}(0)\approx 1$. For large correlation lengths, that is, small values of ξ^2, the slope is thus proportional to $\beta\Sigma$. The temperature independence of the slope thus implies that the Cahn-Hilliard square-gradient coefficient is a well behaved function of the temperature. According to Eq. (10), for small k values, the quotient of the slope and the intercept equals the squared inverse correlation length, ξ^2. The values for the correlation lengths thus obtained are plotted in Fig. 4 as a function of the temperature on a double logarithmic scale. The drawn line is a linear fit according to Eq. (13) with a critical temperature of 17.95 °C. We obtain for the critical exponent, $\nu=0.522\pm0.023$, which corresponds to the expected mean-field value of $\frac{1}{2}$. For the prefactor ξ_0^{-1} we obtain a value of 190 ± 10 nm, which seems quite plausible in view of the diameter of the particles, which is 78 nm.

In Fig. 5 the reciprocal slopes of Fig. 3 are plotted as a function of ξ^2. As pointed out in the theoretical section [see Eq. (10)], we obtain a value for $\beta\Sigma$ from the quotient of the slope and the intersection of this curve, provided that $S_{nc}^{eq}(0)\approx 1$. The value for $\beta\Sigma$, scaled on R_V^2, is found to be equal to 3.60 ± 1.10. The range R_V of the pair potential is taken equal to the particle diameter. This estimated value for $\beta\Sigma/R_V^2$ is larger than the theoretical order of magnitude estimate of 0.1. This is not a bad correspondence, in view of the fact that both the experimental and theoretical values are crude estimates.

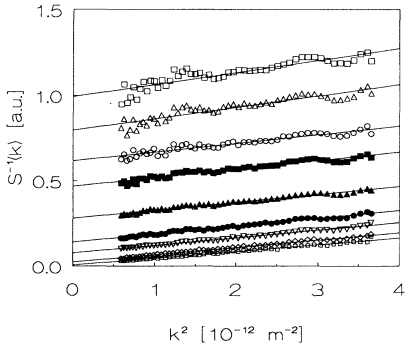

FIG. 3. Reciprocal structure factors plotted as a function of k^2. The quotient of the intercept and slope gives ξ^2. The different temperatures are (from top to bottom): 18.05 °C, 18.10 °C, 18.14 °C, 18.24 °C, 18.34 °C, 18.45 °C, 18.56 °C, and 18.66 °C.

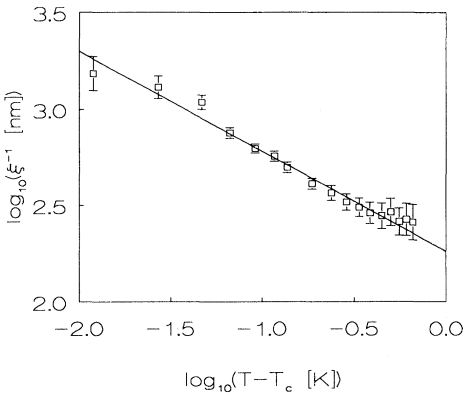

FIG. 4. Correlation lengths obtained from the reciprocal structure factor (see Fig. 3). The solid curve corresponds to a critical exponent of 0.522.

A second way to obtain the temperature dependence of the correlation length is via the turbidity. Figure 6 is a plot of the turbidity versus the temperature. The drawn line is a fit according to Eq. (12) in combination with Eq. (13). Only data points farther away from the critical point than 0.2 °C are taken into account. Multiple scattering, peaked in forward directions, becomes important on approach of the critical point, and probably causes deviations of the turbidity from the theoretical curve for $T-T_c<0.2$ °C. The critical exponent obtained from this fit is 0.511 ± 0.27, which is in agreement with the one obtained via structure factor measurements. This fit turned out to be very insensitive to the value of the prefactor of the exponent in Eq. (13).

B. Shear rate dependence of the turbidity

In Fig. 7 the difference of the turbidity in the sheared and quiescent system is plotted as a function of the shear rate for several temperatures. Close to the critical point

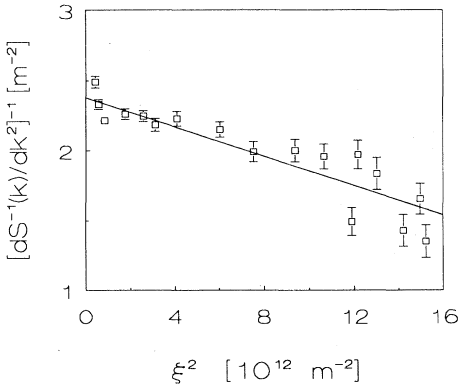

FIG. 5. Reciprocal slopes of Fig. 3 as a function of the reciprocal squared correlation length (ξ^2), used for the determination of $\beta\Sigma/R_V^2$ (see text).

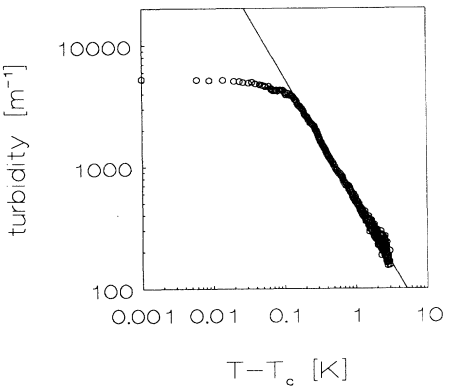

FIG. 6. Turbidity as a function of the temperature. The drawn line is a fit according to Eq. (12) in combination with Eq. (13).

($T-T_c<0.2$ °C), the equilibrium turbidity must be obtained from extrapolation of the straight line in Fig. 6. The effect of shear flow is small at higher temperatures but increases dramatically on approach of the critical point. In that case only a very small shear rate is needed to cause a significant decrease of the turbidity.

In Fig. 8 the data of Fig. 7 are scaled on the turbidity scaling function (7a). To this end, all the turbidity data are plotted as a function of $\dot{\gamma}\xi^{-4}$. The two proportional constants which relate $\tau(\dot{\gamma})-\tau^{eq}$ to $T(\lambda)$ and $\dot{\gamma}\xi^{-4}$ to λ [see Eqs. (6) and (5)] are chosen in such a way that the theoretical curve and the data points have the most overlap. First of all, this figure shows that the $\dot{\gamma}\xi^{-4}$ scaling is satisfied to within experimental error, since all data points given in Fig. 8 collapse onto the same curve. Secondly, the two proportionality constants mentioned above can be chosen such that all data match with the theoretical curve. This verifies the predicted functional dependence of $\tau(\dot{\gamma})-\tau^{eq}$ on $\dot{\gamma}\xi^{-4}$.

We can go a step further, and compare the two proportionality constants between $\tau(\dot{\gamma})-\tau^{eq}$ and $T(\lambda)$, and between $\dot{\gamma}\xi^{-4}$ and λ, with the theoretical values in Eqs. (6) and (5). For the $\dot{\gamma}\xi^{-4}$ axis we used a proportionality constant equal to 5.0×10^{26} s m^{-4}. This constant should equal $1/[2D_0(\beta\Sigma/R_V^2)R_V^2]$, with $D_0=k_BT/6\pi\eta a$,

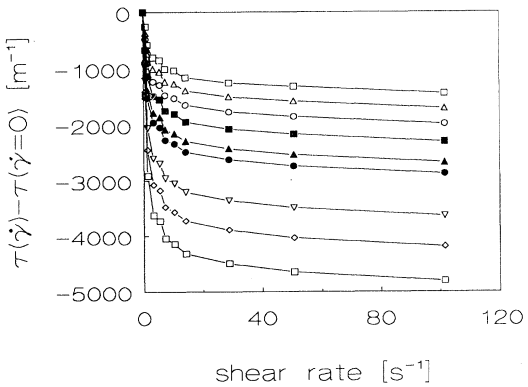

FIG. 7. The turbidity in the system minus the turbidity in the equilibrium state plotted as a function of the shear rate. The different temperatures equal (from top to bottom): 18.41 °C, 18.35 °C, 18.30 °C, 18.25 °C, 18.21 °C, 18.18 °C, 18.10 °C, 18.06 °C, and 18.01 °C.

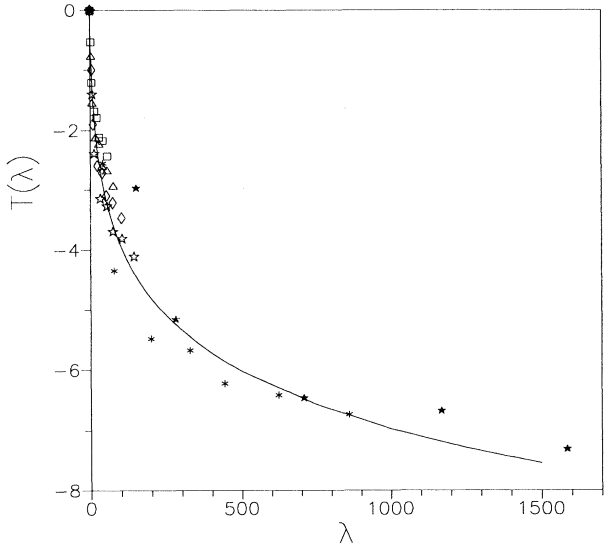

FIG. 8. Data of Fig. 7, plotted against $\dot{\gamma}\xi^{-4}$. The proportionality constants for the λ axis and T axis are chosen in such a way that the data points are best mapped on the theoretical turbidity scaling function.

$\eta=0.652\times10^{-3}$ Pa s (viscosity of benzene at a temperature of 18 °C), $k_BT=4.02\times10^{-21}$ Nm, $a=39$ nm, $R_V=78$ nm, and $\beta\Sigma/R_V^2=3.60$. The constant calculated on the basis of these values is 2.72×10^{24} s m^{-4}. This indicates that the measured values are too large. Three reasons may account for this difference. Firstly, the experimentally obtained value for $\beta\Sigma/R_V^2$ of 3.60 ± 1.10 is noting but a crude estimate, since we assumed $S_{nc}^{eq}(0)\approx1$. Secondly, hydrodynamic interactions are not taken into account in our theory. Hydrodynamic interactions are probably accounted for by replacing D_0 by an "effective diffusion coefficient," which may be much smaller than D_0. Thirdly, the improved closure relation that is used to express the three-particle correlation function g_3 in Eq. (1) in terms of the pair-correlation function g is an approximation. Although this closure relation accounts for the relevant physical phenomena, it may not be correct quantitatively, and contribute to the discrepancy between the measured and the calculated proportionality constant.

The prefactor used for the turbidity axis is 2.10×10^{-3} m. This value should resemble $[(k_0R_V)^2(\beta\Sigma/R_V^2)]/C$. Using a value of 1.42 for the refractive index of the particles and 1.50 for the solvent, this factor is 1.81×10^{-3} m, which is satisfactory in view of the uncertainty in $(\beta\Sigma/R_V^2)$.

V. SUMMARY AND CONCLUSIONS

The effect of shear flow on long-ranged microstructure of a suspension near its gas-liquid critical point is studied by means of turbidity measurements. The colloidal system that we used consists of amorphous silica spheres coated with stearyl alcohol chains. The solvent is benzene, which is a poor solvent for stearyl alcohol, resulting

in attractive interactions between the colloidal spheres, giving rise to an upper-critical gas-liquid critical point.

The shear rate and temperature dependence of the turbidity is found to scale with $\dot{\gamma}\xi^{-4}$ ($\dot{\gamma}$ is the shear rate and ξ^{-1} the temperature dependent correlation length of the quiescent suspension), in accord with the mean-field theoretical prediction. The correlation length is found to diverge with the mean-field exponent $\frac{1}{2}$ for $T-T_c > 0.05\,^{\circ}\mathrm{C}$. The functional dependence of the turbidity on $\dot{\gamma}\xi^{-4}$ is also verified, although there is some uncertainty concerning the proportionality constant relating the turbidity to the theoretical scaling function. This uncertainty is due to (i) an inaccurate experimental value for the Cahn-Hilliard square-gradient coefficient, (ii) the neglect of hydrodynamic interactions in the theory, and (iii) the fact that the closure relation that is used to express the three-particle correlation function g_3 in terms of the pair-correlation function g is an approximation.

ACKNOWLEDGMENTS

This work is part of the research program of the Foundation for Fundamental Research of Matter (FOM) with financial support form the Netherlands Organization for Scientific Research (NWO).

[1] J. K. G. Dhont and H. Verduin, J. Chem. Phys. **101**, 6193 (1994).
[2] A. Onuki and K. Kawasaki, Ann. Phys. **121**, 456 (1979).
[3] D. W. Oxtoby, J. Chem. Phys. **62**, 1463 (1975).
[4] D. Beysens, in *Scattering Techniques Applied to Supramolecular Nonequilibrium Systems,* edited by Sow-Hsin Chen, Benjamin Chu, and Ralph Nossal, Vol. 73 of *NATO Advanced Study Institute, Series B: Physics* (Plenum, New York, 1981), p. 411.
[5] D. Beysens and M. Gbadamassi, Phys. Rev. A **22**, 2250 (1980).
[6] J. K. G. Dhont and A. F. H. Duyndam, Physica A **189**, 532 (1992).
[7] V. G. Puglielli and N. C. Ford, Jr., Phys. Rev. Lett. **35**, 143 (1970).
[8] A. K. van Helden, J. W. Jansen, and A. Vrij, J. Colloid Interface Sci. **81**, 352 (1981).
[9] A. Einstein, *Investigations on the Theory of the Brownian Movement,* edited by R. Fürth (Dover, New York, 1956).
[10] P. W. Rouw and C. G. de Kruif, J. Chem. Phys. **88**, 7799 (1988).
[11] H. Verduin and J. K. G. Dhont, J. Colloid Interface Sci. (to be published).
[12] S. J. Johnson, C. G. de Kruif, and R. P. May, J. Chem. Phys. **89**, 5909 (1988).